LA-UR-15-20073 (Accepted Manuscript)

Modelling hepatitis C therapy—predicting effects of treatment

Perelson, Alan S.
Guedj, Jeremie

To be published in: Nature Reviews Gastroenterology & Hepatology

DOI to publisher's version: 10.1038/nrgastro.2015.97

Permalink to record: http://permalink.lanl.gov/object/view?what=info:lanl-repo/lareport/LA-UR-15-20073

Use of Modeling in Hepatitis C Therapy: Predicting Future Effects of Treatments Now

Alan S Perelson[1*] and Jeremie Guedj[2,3]

[1]Theoretical Biology and Biophysics, MS-K710, Los Alamos National Laboratory, Los Alamos, NM 87545 USA

[2] IAME, UMR 1137, INSERM, F-75018 Paris, France

[3] IAME, UMR 1137, Univ Paris Diderot, Sorbonne Paris Cité, F-75018 Paris, France

*Corresponding author. Email : asp@lanl.gov; telephone : 505-667-6829 ; fax 505-665-3493

Abstract (200 words)

Mathematically modeling the changes in HCV RNA measured in infected patients during antiviral therapy has yielded many insights into HCV pathogenesis and the effects of treatment. By determining how rapidly HCV is cleared when HCV replication is interrupted by antiviral therapy one can deduce how rapidly HCV is produced before therapy in patients maintaining a constant baseline HCV RNA level. This knowledge coupled with estimates of the HCV mutation rate allows one to estimate the frequency at which drug resistant variants arise. Modeling has also allowed one to deduce the effectiveness of an antiviral agent in blocking HCV replication from the magnitude of the initial, i.e. first phase, viral decline, to estimate the lifespan of an HCV infected cell from the slope of the subsequent, i.e. second phase, viral decline and to estimate the duration of therapy needed to cure infection. Interestingly, some of the lessons learned from modeling HCV RNA declines under interferon-based therapies needed to be revised in order to understand the HCV RNA decline kinetics observed with direct-acting antiviral agents (DAAs). Lastly, we discuss unresolved issues involving understanding therapies with combinations of DAAs such as whether a sustained virological response necessarily involves elimination of all infected cells.

Review Criteria: The focus of this review is the use of mathematical modeling in hepatitis C therapy with particular regard to new therapies. As such, we relied on PubMed as well as various previously published reviews and articles in the modeling and clinical literature that focused on viral kinetics, estimating effectiveness of therapy and determining the duration of therapy.

Key Points:

1) After patients are put on potent therapy, HCV RNA declines in a biphasic manner with the first phase reflecting the clearance of virus and the second phase reflecting the loss of infected cells.
2) The magnitude of the first phase decline is a direct measure of the effectiveness of therapy in reducing viral production from infected cells, with a one log decline corresponding to a 90% effectiveness, a two log decline a 99% effectiveness and so on.
3) Modeling the HCV RNA declines under therapy has allowed researchers to estimate the rate of HCV clearance from the circulation, the rate of HCV production and the needed duration of therapy needed to eliminate the last infectious agent. The best current estimates are that the HCV half-life is 45 minutes and that approximately 10^{12} virions are produced each day in a chronically infected patient. At this rate of production all single and double mutant variants are produced daily allowing rapid drug resistance to emerge when therapies with low genetic barriers are employed.
4) Multiscale models that model intracellular events of viral replication and release as well as extracellular spread of virus have shown that NS5A and protease inhibitors have multiple models of action and can inhibit both viral replication and viral assembly or release.
5) Interferon-free combination therapies are available now, show little resistance and are able to generate sustained virologic responses after treatments as short as 6 weeks.
6) With some DAA combinations, HCV RNA has been detected at the end of treatment in patients that go on to develop a sustained virologic response. Viral kinetic theory cannot explain this and new theory may need to be developed for some combination DAA therapies.

Introduction

The field of hepatitis C virus (HCV) research and treatment has entered a new era with the advent of direct acting antivirals (DAAs) that are safe, orally deliverable and able with a short treatment duration to cure HCV infection in nearly every patient. Some of the rapid advances in the development of new therapeutics have their basis in mathematical modeling, which provided tools to rapidly assess the in vivo effects of new antivirals. Terms such as the first and second phase of viral decline went from being mathematical characterizations of viral kinetics to phrases familiar to almost all researchers and clinicians in the field. This review will be focused on providing insights into these developments as well as show how the early concepts developed by studying patient responses to interferon (IFN)-based therapies have had to change in order to understand the effects of DAA-based therapies. Further, as we look to the future, we all want to know how short the period of treatment can be made when combinations of DAAs are used. Will it be possible to cure some individuals with four weeks or two weeks of treatment? What are the barriers to rapid cure? How can we evaluate whether a patient is on track to be cured rapidly or if longer treatment durations are needed? While these questions will not be directly answered here, the concepts needed to provide answers will be discussed.

The basis and principles of viral kinetic modeling determined from IFN-based therapy

Dynamic equilibrium in absence of treatment

One of the most important insights of viral kinetic modeling has its origins in earlier work involved with modeling the effects of antiretroviral treatment on HIV[1-4] . It is based on the simple heuristic argument that a change in viral load reflects an imbalance between the antagonistic processes of viral production and clearance. This can be written mathematically as

$$\frac{dV}{dt} = pI - cV \quad , \quad (1)$$

where V is the viral load, dV/dt is its rate of change, p is the rate of viral production per infected cell, I, and c is the per virion rate of viral clearance (i.e., the virion half-life is ln(2)/c). During chronic infection, the viral load is stable and remains roughly equal to a set-point level denoted V_0. At the set-point, and the rates of viral production and viral elimination balance so that $pI_0=cV_0$, where the set-point number of infected cells is I_0.

The first phase of viral decline

The initiation of anti-HCV treatment disrupts the equilibrium between the virus and the host. Most antivirals (such as IFN or DAAs) act by blocking viral production and thus reduce p, say by a factor (1-ε), where ε is the effectiveness of therapy that varies between 0 and 1, with 1 representing a 100% effective therapy. Neumann et al.[5] showed that Eq. (1), with p replaced by (1- ε)p , predicted that the viral load will fall according to the equation

$$V(t) = V_0(1 - \varepsilon + \varepsilon e^{-ct}) \qquad (2)$$

for a short period of time after the initiation of therapy during which the viral production rate pI remains approximately constant and equal to pI_0. The exponential term in Eq. (2) approaches 0 as time proceeds, thus the viral load will decline to the value V_0(1-ε), reflecting that treatment leads to lower levels of viral production. What this implies, is that if a drug is 99% effective then the viral load should fall to 0.01 V_0. Thus, the theory tells us that one can read off the effectiveness of a drug that blocks viral production by the $\log_{10}$ viral decline it causes, i.e. if a drug causes a 2 $\log_{10}$ decline then it is 99% effective.

Neumann et al.[5] used this model to fit viral load data obtained from genotype 1 HCV-infected patients treated with different doses of IFN-α and sampled very frequently after drug therapy was started. After a delay of about 8 hrs, reflecting the time needed for IFN to bind to cellular receptors and cause upregulation of interferon-stimulated genes (ISGs)[6], HCV RNA declined rapidly for the first day (Fig. 1a), with a clearance rate $c \sim 6$ d^{-1} corresponding to a half-life of HCV in the circulation of about 2.7 hours[5]. Further, the extent of decline was IFN-dose dependent corresponding to a dose dependent effectiveness in blocking viral production[5]. Importantly, if HCV is rapidly eliminated from serum it implies that large quantities of virus need to be produced every day (about 10^{11}-10^{12} virions) to maintain set-point viral levels of 10^6-10^7 HCV RNA copies/mL in the absence of treatment.

The second phase of viral decline

After day 2, viral load does not plateau, as predicted by Eq. (2), but rather continues to decline, although with a slower rate (Fig. 1b). This failure of Eq. (2) to continue to correctly predict the kinetics of viral decline reflects the fact the rate of viral production begins to decline

as infected cells die and are not efficiently replaced due to the fact that the viral load has declined during the first phase. As the number of newly infected cells declines, overall viral production is further reduced. Therefore, the effect of treatment, even if modest, triggers a fatal circle of events that leads to a continuous decline of virus and infected cells, called the second phase, which continues as long as treatment is maintained. Mathematical analysis[5] reveals that the rate of this decline is approximately equal to $\delta\varepsilon$, where δ is the loss rate of infected cells. For potent drugs, where $\varepsilon \sim 1$, the second phase slope is to a good approximation δ.

Extended models

Although the biphasic model gives the basic foundation for understanding the determinants of early viral decline, more complex models have been introduced to understand the role of liver regeneration and the effects of ribavirin (RBV) and drug pharmacokinetics[7-22]. The putative effects of RBV have been extensively reviewed elsewhere[8,9,23-27] and will not be discussed here.

Liver regeneration

An important prediction of models taking into account hepatocyte proliferation is the existence of a threshold, called the "critical drug effectiveness" and noted ε_c . If $\varepsilon<\varepsilon_c$, the virus is not eradicated sufficiently rapidly and the progressive replenishment of target cells over time allows the remaining virus to infect new cells and establish a new (lower) set-point in spite of ongoing therapy. Interestingly, mathematical analysis of these models reveals that the value of ε_c depends on and increases with parameters that determine the baseline HCV RNA and the proportion of infected cells[16], thus possibly explaining why high baseline viral loads and presence of advanced fibrosis are negatively correlated with SVR[28].

Drug pharmacokinetics

Viral rebound can be due to a loss of drug effectiveness over time due to lower drug concentrations towards the end of the dosing period as sometimes seen with weekly administration of pegylated IFN [7,11,17]. The relationship between drug concentration and antiviral effectiveness in blocking viral production can be described by a so called E-max model:

$$\varepsilon(t) = \frac{E_{max}\, C(t)^n}{EC_{50}^n + C(t)^n} \quad (3)$$

where *C(t)* is the drug concentration at time *t*, EC_{50} is the drug concentration needed to achieve an effectiveness of 50% of the maximum effect, E_{max}, and *n* is a constant called the Hill coefficient, a parameter that determines the steepness of the drug concentration–effect curve[20,29]. Because drug concentrations are not always available, more empirical models have also been proposed to describe the patterns of change in drug effectiveness over time[30,31], such as an exponential model for drugs whose concentrations decay or build up over time:

$$\varepsilon(t) = \varepsilon_1 + (\varepsilon_2 - \varepsilon_1)(1 - e^{-k_\varepsilon t}) \quad (4)$$

where the treatment effectiveness starts from an initial level, ε_1, changes to a final level, ε_2, with k_ε representing the rate of change of effectiveness. Thus, if $\varepsilon_2<\varepsilon_1$ the model can mimic the effect of a decrease in drug effectiveness over time, as observed for instance towards the end of the dosing interval with weekly Peg-IFN[30,32]. Conversely, if $\varepsilon_2>\varepsilon_1$ the model can mimic the effect of an increase in drug effectiveness over time, as it is the case with some DAAs where the short drug half-life or the time to achieve high levels of active metabolites may induce a delay until the drug is fully effective [29,33-36] [22,37].

Summary

Although the models inherited from IFN-based therapy have proven useful in analyzing the early changes in viral load decay with IFN and some DAAs, they are limited by the fact that the effect of treatment simply consists of blocking production of drug-sensitive virus. In order to understand the various patterns observed during DAA treatment, such as the origin of the accelerated viral decay or the emergence of resistance to treatment, one needs to use more complex models that take into account the various stages of viral replication targeted by DAAs and/or account for the emergence of resistance to treatment.

Viral kinetics with DAAs

The fast first phase and the effect of some DAAs in blocking virion assembly/secretion

Because the NS5A protein has no enzymatic functions, the effect of blocking NS5A has been poorly understood. Using an innovative screening approach the NS5A inhibitor daclatasvir was identified and showed that NS5A could be an important target for anti-HCV treatment[38]. From a modeling point of view, the viral kinetics observed under daclatasvir therapy were particularly interesting and revealed a first phase of viral decline that was much faster than seen with previous treatments[38,39]. In fact, Gao et al.[38] showed that HCV RNA could decline by 3 logs 12 hrs after a single dose of daclatasvir, from which it was deduced that HCV RNA was cleared from the circulation with a half-life of 45 min[39] and not with the previously estimated 2-3 hr half-life[5,40]. Guedj et al.[39] hypothesized that if NS5A inhibitors potently blocked both viral secretion and viral replication, then viral load would fall more rapidly than with therapies that mainly blocked viral replication. If a therapy mainly interfered with viral replication, then viral RNA present within infected cells when therapy was started could continue to be packaged into virions and exported after drug therapy was initiated. If this were the case, then viral production would continue leading to an underestimate of the rate of viral clearance.

In order to characterize more precisely the effect of daclatasvir, Guedj et al.[39] developed a multiscale model that could be used to analyze clinical data (Fig. 2). An importance feature of this model was that the number of viral RNA molecules, $R(a,t)$, within an infected cell were modeled as a function of the length of time, a, they had been infected and the time t they had been exposed to therapy. Within the infected cell viral RNAs accumulate as they are synthesized and decrease in number as they are degraded or assembled into virions which are then secreted. The Guedj et al. model thus included the drug effectiveness in blocking viral production, ε_α, the drug effectiveness in blocking viral assembly/secretion, ε_s, and its effectiveness in modulating the rate of viral RNA degradation, κ (i.e., $\kappa>1$ if a drug enhances the rate of viral RNA degradation). Converting the multiscale model into a set of equations is a complicated matter and mathematical formulation and analysis of the model can be found in a number of recent publications [39,41,42].

Using this model to fit the viral decline during the first two days after administration of IFN and daclatasvir, Guedj et al.[39] suggested that the latter had a dual mode of action and efficiently blocked not only vRNA production, with $\varepsilon_\alpha=0.99$, but even more profoundly inhibited virus assembly/secretion ($\varepsilon_s=0.998$). Daily IFN was predicted to have a small effect on

assembly/secretion (ε_s=0.39) and its main effect at doses of 10 and 15 MU was on viral replication (ε_α=0.96). In separate analyses, it was also found that the protease inhibitors telaprevir (ε_s=0.95)[39] and danoprevir (ε_s=0.56)[41] had an inhibitory effect on virion assembly/secretion but the effect was not as profound as daclatasvir's. This may explain why the virion clearance rate estimated for patients treated with telaprevir[34,44] was higher that of patients treated with IFN[33,43] but not as high as for those treated with daclatasvir[39]. Interestingly, the predictions that NS5A inhibitors and protease inhibitors affect both viral replication and virion assembly/secretion are now supported by *in vitro* experiments[39,44,45]. In addition, Meredith et al.[46] recently showed that IFN can rapidly affect infectious particle genesis.

The intracellular model used in the multiscale model (Fig. 2) is simplistic. More complex models of intracellular replication have been developed[47,48] but utilizing them to fit clinical data within the context of a multiscale model remains challenging.

The fast second phase and the possibility of curing infected cells

Although standard viral dynamic models initially attributed the second phase of viral decline to infected cell death[5,40,49], the faster second phase observed with many DAAs and particularly protease inhibitors[33,41,43,50] called this assumption into question. A more plausible assumption is that intracellular penetration of highly effective drugs leads to cure of infected cells, i.e. causes the loss of intracellular viral RNA as has been observed in the replicon system with high doses of IFN[51,52]. In addition, some DAAs, in particular protease inhibitors, may also help restore innate immune responses within infected cells and these responses may contribute to a faster loss of intracellular viral RNA[53]. However, whether their concentrations in vivo are high enough to generate this affect has been questioned[54].

Interestingly, nucleos/tide polymerase inhibitors have so far not shown such fast second phase declines[35,55]. For example, the viral declines induced by the HCV polymerase inhibitor sofosbuvir alone or in combination with ribavirin or another nucleotide analogue have been modeled [35,56] and δ was estimated to 0.2-0.3 d^{-1} in naïve patients. This is faster than the 0.14 d^{-1} seen on average with IFN-based therapies[5,49] but slower than the 0.5-0.6 d^{-1} observed with telaprevir monotherapy or in combination with Peg-IFN in naïve patients [33] (Fig. 3). Although it was suggested that a correlation may exist between a high antiviral effectiveness and a fast

second phase[33,57,58], the slower second phase with sofosbuvir than telaprevir was obtained despite a higher sofosbuvir effectiveness in blocking viral production (median $\varepsilon = 0.9996$ for sofosbuvir vs. 0.999 for telaprevir), suggesting that the mode of action of the drug may play a role in this correlation.

The possibility that the fast second phase declines seen with protease inhibitors might be due to cure of infected cells led Guedj and Neumann to propose a model including the effect of drug on intracellular viral replication. Their model incorporated both positive strand HCV RNA and replication complexes within infected cells and showed that drugs leading to a continuous loss of replication complexes at rate γ, would generate an accelerated second phase of viral decline with slope $\delta+\gamma$[59]. Thus, the model predicted that the second phase was due to the combined effect of infected cell death and lower levels of viral replication in the remaining infected cells.

The majority of viral kinetic analyses of DAA-based treatments have been done for treatment naïve non-cirrhotic patients. Results obtained in studies involving small populations found a much slower second phase of viral decline in cirrhotic or treatment experienced patients [58,60]. More data are needed to precisely evaluate the effect of host characteristics, such as fibrosis stage and IL28B polymorphism, and virus genotype on viral kinetics during DAA therapy.

Implications for treatment duration

Regardless of its origin, having a more rapid second phase should allow for shorter treatment duration. In order to predict the time needed to eradicate HCV, Dixit et al.[9] introduced a theoretical threshold, now called a "cure boundary"[49]. This cure boundary was defined as having less than one viral particle in the extracellular body fluid, i.e. 15 L, and corresponds to the unobservable concentration of $10^{-4.22}$ IU/mL. Using this cure boundary, eradication requires the viral load to decline > 10 $\log_{10}$ from a typical baseline of 10^6 IU/ml[9]. With current assay limits of detection of about 10 IU/mL there is are still another 5 logs or so of decline needed before the viral load hits the cure boundary (Fig. 4a). Other authors have defined the cure boundary as having less than one infected cell, which is a slightly more conservative assumption and delays the predicted time to eradication by 2-3 weeks with standard parameter values [33,49].

Using the concept of a cure boundary, treatment duration can easily be predicted from the first and second phases of viral decline. Using the rapid viral decline in patients treated with danoprevir, a protease inhibitor, and mericitabine, a polymerase inhibitor, this approach led Gane et al.[61] to predict that between 8 and 12 weeks of treatment should be sufficient to cure patients treated with DAAs. About the same time, by simulating a clinical trial in which patients first and second phase declines were chosen at random from the parameter distributions estimated in patients treated with telaprevir, Guedj and Perelson[33] concluded that 95% of patients could obtain SVR (defined as having less than one virion remaining) in 7 weeks, assuming that the patients complied with their therapy and that the predicted second phase decline continued unchanged when it is below the limit of detection (Fig. 4b)[33]. This would be the case only if the treatment has a sufficiently high genetic barrier to resistance and there are no viral reservoirs. In fact, SVR rates obtained after 12 or 24 weeks of treatment with danoprevir and mericitabine were low, and virologic breakthrough or relapse were associated with danoprevir-resistant virus in most cases[62]. Similarly, the prediction of 7 weeks of therapy to obtain 95% SVR would not apply to telaprevir monotherapy but rather to some combination DAA therapy, which would prevent resistance development, and which had the kinetic characteristics observed during short-term telaprevir therapy.

Interestingly, several clinical trials have now validated the prediction that SVR can be achieved in a large fraction of non-cirrhotic treatment naïve patients with 8 weeks of treatment or less with some DAA combinations[63-65]. In the ION-3 trial, among previously untreated genotype 1 patients without cirrhosis SVR12 was 94% after 8 weeks of treatment with sofosobuvir and ledipasvir[63]. In the C-WORTHY trial, among previously untreated HCV genotype 1a patients given grazoprevir (MK-5172) and elbasvir (MK-8742) for 8 weeks, SVR12 was 80%[64]. Lastly in the SYNERGY trial, among treatment naïve genotype 1 patients given 6 weeks of sofosobuvir, ledipasvir and either GS-9669 (a non-nucleoside NS5B inhibitor) or GS-9451 (an NS3/4A protease inhibitor) SVR12 was 95%[65].

The combination of a cure boundary and more complex viral kinetic models, some incorporating drug pharmacokinetics, have been used to predict SVR rates with different dosing regimens[49,57,66,67]. For instance N'Guyen fitted the viral kinetics observed in patients treated for 4 weeks with alisporivir (a cyclophylin inhibitor) or alisporivir/peg-IFN. Then they used the model

to accurately predict the SVR rate of a subsequent clinical study with a 24 week treatment duration and a complex response-guided design, showing that modeling of short-term data can be used to anticipate the outcome of a complex clinical trial[21].

Modeling drug resistance

As explained above due to the emergence of drug resistant variants the second phase of viral decline may not be sustained and the treatment duration predicted from the second phase may not be accurate. In fact, viral breakthrough due to resistance was shown to occur as early as 2 days after initiation of telaprevir monotherapy[68], with between 5 and 20% of clones sequenced carrying known resistance mutations. Further, virus rapidly rebounded and by the end of therapy at day 14 almost all virus was drug resistant[68]. Using the facts that HCV has a high daily production rate[5] and a high error rate during replication[69,70], Rong et al. calculated that all viable single and double mutant resistant viruses may exist before treatment and compete with wild-type virus during therapy[71]. This led them to predict that only treatments with a high genetic barrier to resistance can lead to SVR[71]. Since viral competition plays a critical role in determining long term viral decline, mathematical models have been expanded to account for drug-sensitive and drug-resistant virus[71], or wild-type plus multiple viral strains[57,72,73].

The mechanism underlying the rapid rebound of resistant virus is not fully understood. To grow, resistant virus needs "replication space". In some models the rapid expansion of mutant virus is supported by the infection of newly produced hepatocytes[71,72]. However this assumption remains to be validated as little data is available on hepatocyte kinetics. Replication space could also be supplied by other mechanisms, such as reinfection of cells previously infected with wild-type virus, superinfection of already infected cells or the loss of an antiviral state due to lower viral levels. Understanding the mechanism of resistant virus expansion and subsequent treatment failure may provide new insights into the design of better combination therapies targeting both the host and the virus.

Summary

Multiscale models have provided a novel understanding of the origin of the early rapid viral decline with DAAs. However, an appropriate combination of potent, well-tolerated DAAs needs to be used to avoid resistance and lead to shorter treatment durations.

Predicting Future Effects of Treatments Now

Modeling potent drug combination in vivo: a simple extension of existing models?

In the future, most treatments for HCV will involve IFN-free combinations of DAAs. Standard or multiscale models can be expanded to account for drug combinations using pharmacological concepts of drug additivity and synergy[74,75] or by simply analyzing the HCV RNA decline kinetics and estimating the overall effectiveness of the combination therapy. From a modeling perspective, two of the more interesting recent DAA clinical trials were the SPARE trial[56] in which 60 treatment naïve mostly genotype 1 patients were given 400 mg daily of sofosbuvir plus ribavirin (SOF+RBV) for 24 weeks and the SYNERGY trial[65], in which 60 treatment naïve patients mostly infected with genotype 1 HCV were randomized 1:1:1 to sofosbuvir and ledipasvir for 12 weeks (SOF+LDV, Arm A), SOF+LDV plus the non-nucleoside polymerase inhibitor GS-9669 for 6 weeks (Arm B) or SOF+LDV plus polymerase inhibitor GS-9451 for 6 weeks (Arm C). The viral load decline in all three arms of the SYNERGY trial was initially more rapid than in patients treated with SOF + RBV, which can be attributed to a high effectiveness of the NS5A inhibitor LDV in blocking viral assembly/secretion. However, by day 3 and subsequently, patients treated with SOF+RBV achieved largely comparable levels of virus as the patients in all arms of SYNERGY suggesting that

i) In spite of an additive effect in vitro[76], SOF+LDV did not have a larger effect in blocking viral RNA production in vivo than SOF+RBV.

ii) The possibility of shorter treatment with SOF+LDV was not due to faster kinetics of viral decline.

Further, based on the observed viral decline kinetics in arms B and C of SYNERGY, one would predict an SVR rate between 7% and 26% (based on eliminating the last virus particle after six weeks of treatment) and not the 95% observed [65].

Can we still use HCV RNA as a reliable biomarker of treatment efficacy?

Another unexpected and remarkable finding in arms B and C of the SYNERGY trial was that at the end of treatment, i.e. week 6, 12 out of 20 patients (60%) in arm B and 10 out of 20 (50%) in arm C, had detectable HCV RNA levels, i.e. above the 3 IU/ml detection limit of the highly sensitive Abbott real time HCV assay[65]. As explained above, having HCV RNA close to

the detection limit implies that viral eradication is still far off; in fact, standard tools of mathematical modeling would predict that there are still about one million virions produced every day[5]. Consequently, all existing HCV models would predict that patients with detectable viremia would progressively rebound as active intracellular drug decayed after the EOT. But in SYNERGY only one patient in arm B exhibited rebound (and one patient in arm C was lost to follow up after reaching SVR4). Thus the notion of a cure boundary corresponding to the loss of the last viral particle or last infected cell at the EOT does not appear to be a valid criterion for cure with these DAAs. This is not an isolated incident. Sarrazin et al.[77] recently noted that in a phase 2a trial (PILOT study) in which 11 patients received the NS3 protease inhibitor ABT-450 co-dosed with low dose ritonavir and the non-nucleoside NS5B polymerase inhibitor ABT-072 and RBV for 12 weeks, residual viremia was detected by the Abbott real time HCV assay in three patients who achieved SVR as late as therapy weeks 9, 10 and 12. These observations, as well as others[78], also raise the issue of whether HCV RNA levels at the EOT can be used for clinical decision making. At the moment, there is no proven explanation for the lack of viral rebound in patients with detectable HCV RNA at the EOT, but the two obvious possibilities are that the immune system is controlling the virus leading to a functional cure, as has been reported in rare instances in HIV-infected patients taken off therapy[79], or that the HCV RNA detected by the Abbott assay was not infectious.

A related concern has been the phenomenon of late relapse. Lawitz et al.[80] noted that in a small phase 2a trial involving 11 subjects given 2 DAAs (ABT-450/r and ABT-072) plus RBV for 12 weeks, one patient relapsed at post-treatment week 36 with a virus most likely representing the baseline strain based on sequence analysis. There have been other scattered reports of very late relapse[81,82], possibly supporting the idea of breakthrough from immune control or the existence of viral reservoirs. Consistent with an important role of the immune system, trace amounts of HCV RNA were sporadically found in plasma up to 8 years after successful therapy[83].

More data are needed to assess whether other DAA combinations give rise to the same phenomenon and whether clinical algorithms of treatment duration based on time to achieve undetectable viremia need to be revisited for the new combination treatments. Given the possible importance of the immune system in the control of the infection, incorporating immunological data such as anti-HCV antibodies or cytokines, such as interferon γ–induced protein 10 (IP-10)

levels, may be helpful in order to improve SVR prediction with new DAA combinations. For instance, it was recently suggested that IP-10 kinetics may be used as a surrogate marker of the rate of intracellular viral replication complex decay[84], and thus may help characterize the kinetics of cell cure.

Summary

Some data obtained with DAAs call into question the simple notions of a cure boundary based on eliminating the last virus or productively infected cell and suggest that SVR does not necessarily require complete viral eradication at the end of treatment.

Conclusions

Mathematical models have played an important role in deciphering the kinetics of viral decline during anti-HCV drug therapy, leading the FDA to recommend its use during drug development[85]. The magnitude of the first phase of viral decline has been used to determine the antiviral effectiveness of drugs that block HCV replication in very short-term clinical trials. New developments, such as the multiscale model, have been used to gain further information into the modes of action of new antivirals and determine whether antivirals block virion assembly/release, block HCV RNA replication or enhance the degradation of intracellular HCV RNA. Models have also led to the idea of a cure boundary, which has proven useful for determining the length of interferon-based therapies. With some new combinations of DAA, high SVR rates have been obtained after 6-12 weeks of therapy, with some patients having a slow kinetics of viral decline and detectable HCV RNA at the end of therapy or very late relapses, suggesting that new models are needed to comprehend the in vivo interactions between DAAs and their effect on viral eradication.

Acknowledgments. This work was performed under the auspices of the U.S. Department of Energy under contract DE-AC52-06NA25396, and supported by NIH grants R01-AI028433, R01-HL109334, R01-AI078881, and the National Center for Research Resources and the Office of Research Infrastructure Programs (ORIP) through grant R01-OD011095.

Competing Interests. Both authors have been consultants for Gilead Sciences. ASP also consults for Bristol-Myers Squibb and Achillion Pharmaceuticals.

Figure Captions.

Figure 1. Viral load decays in a genotype 1 HCV infected patient treated with 15 MIU of IFN-α given daily. (a) The kinetics of the viral decline during the first 2 days of therapy and the best-fit of the model, Eq. (2), (solid line) to the data (solid circles). (b) The viral decline in the same patient over the first 10 days of therapy (solid circles) and the best-fit of the Neumann et al. model[5] that incorporates a second phase decline due to death of infected cells (solid line). Adapted from Neumann et al. Science 282: 103-107 (1998).

Figure 2. Comparison of the standard viral dynamic model (A) with a multiscale model (B). (A) The standard model includes target cells, T, that are produced at rate s (not shown), become infected with rate constant β by interacting with virus and die at per capita rate d. Infected cells, I, produce virus at rate p per cell and die at per capita rate δ. Finally, virus, V, in addition to being produced is cleared at rate c per virion. Treatment acts by reducing the average number of virions produced by an infected cell from p to $p(1-\varepsilon)$. The drug effectiveness, ε, represents a global measure of antiviral effectiveness that does not distinguish among the stages of intracellular viral replication, assembly and release that are blocked by treatment. (B) The multiscale model accounts for intracellular processes involving HCV RNA (vRNA), R, i.e., production, degradation, and assembly/secretion with rate parameters α, μ, and ρ, respectively. The vRNA level within an infected cell (dashed circle) is assumed to increase with time since infection, i.e. the age of an infected cell, a, and ultimately reach a steady state. Treatment (parameters in red) may block vRNA production with effectiveness ε_α, and/or virion assembly/secretion with effectiveness ε_s, and/or enhance the degradation rate of vRNA by a factor κ. Reproduced with permission from Guedj et al. Proc. Natl. Acad. Sci. USA 110: 3991-3996 (2013).

Figure 3. Median viral load decays from baseline (points) and nonparametric kinetic fitting (line) caused by agents belonging to different therapeutic classes during (A) short-term monotherapy or (B) combination therapy. (A). IFN 10 or 15 MIU QD[5] (black), mericitabine 1500 mg BID [55] (green), sofosbuvir 400 mg QD[35] (red), telaprevir 750 mg q8h[33] (blue) and a single dose of daclatasvir (10 or 100 mg, purple)[39]. (B). IFN 10 or 15 MIU QD[5] (black), sofosbuvir 400 mg

QD + RBV (red)[56], telaprevir 750 mg q8h + Peg-IFN[33] (blue) and sofosbuvir 400 mg QD + ledipasvir 90 mg QD[65] (purple).

Figure 4. (a). Illustrative schematic of the cure boundary. The cure boundary may be based on eliminating the last virus particle (orange), eliminating the last infected cell (not shown) or be a threshold beyond which the immune system can contain the infection (blue circle). In addition, when the viral load falls below the limit of quantitation (LOQ) the rate of viral decay can no longer be observed and may change (orange dashed line) due to missed drug doses, emergence of drug resistance, viral reservoirs or other factors and thus influence the time needed to hit the cure boundary. (b). Estimated cumulative probability distribution function for the treatment duration needed to eliminate the last remaining virus particle. The black line corresponds to perfect treatment adherence, whereas the red line represents the case of partial adherence to a regime of three doses per day, where one dose is randomly missed every 2 days. Reproduced with permission from Guedj et al. Hepatology 53: 1801-1808 (2011).

References

1 Ho, D. D. *et al.* Rapid turnover of plasma virions and CD4 lymphocytes in HIV-1 infection. *Nature* **373**, 123-126, doi:10.1038/373123a0 (1995).

2 Perelson, A. S. *et al.* Decay characteristics of HIV-1-infected compartments during combination therapy. *Nature* **387**, 188-191, doi:10.1038/387188a0 (1997).

3 Perelson, A. S., Neumann, A. U., Markowitz, M., Leonard, J. M. & Ho, D. D. HIV-1 dynamics in vivo: virion clearance rate, infected cell life-span, and viral generation time. *Science* **271**, 1582-1586 (1996).

4 Wei, X. *et al.* Viral dynamics in human immunodeficiency virus type 1 infection. *Nature* **373**, 117-122, doi:10.1038/373117a0 (1995).

5 Neumann, A. U. *et al.* Hepatitis C viral dynamics in vivo and the antiviral efficacy of interferon-alpha therapy. *Science* **282**, 103-107 (1998).

6 Dahari, H., Sainz, B., Jr., Perelson, A. S. & Uprichard, S. L. Modeling subgenomic hepatitis C virus RNA kinetics during treatment with alpha interferon. *J Virol* **83**, 6383-6390 (2009).

7 Powers, K. A. *et al.* Modeling viral and drug kinetics: hepatitis C virus treatment with pegylated interferon alfa-2b. *Seminars in liver disease* **23 Suppl 1**, 13-18, doi:10.1055/s-2003-41630 (2003).

8 Herrmann, E., Lee, J.-H., Marinos, G., Modi, M. & Zeuzem, S. Effect of ribavirin on hepatitis C viral kinetics in patients treated with pegylated interferon. *Hepatology (Baltimore, Md.)* **37**, 1351-1358, doi:10.1053/jhep.2003.50218 (2003).

9 Dixit, N. M., Layden-Almer, J. E., Layden, T. J. & Perelson, A. S. Modelling how ribavirin improves interferon response rates in hepatitis C virus infection. *Nature* **432**, 922-924 (2004).

10 Pawlotsky, J.-M. *et al.* Antiviral action of ribavirin in chronic hepatitis C. *Gastroenterology* **126**, 703-714 (2004).

11 Talal, A. H. *et al.* Pharmacodynamics of PEG-IFN alpha differentiate HIV/HCV coinfected sustained virological responders from nonresponders. *Hepatology* **43**, 943-953 (2006).

12 Herrmann, E. *et al.* Viral kinetics in patients with chronic hepatitis C treated with the serine protease inhibitor BILN 2061. *Antiviral therapy* **11**, 371-376 (2006).

13 Dahari, H., Ribeiro, R. M. & Perelson, A. S. Triphasic decline of hepatitis C virus RNA during antiviral therapy. *Hepatology* **46**, 16-21, doi:10.1002/hep.21657 (2007).

14 Dahari, H., Lo, A., Ribeiro, R. M. & Perelson, A. S. Modeling hepatitis C virus dynamics: liver regeneration and critical drug efficacy. *J Theor Biol* **247**, 371-381 (2007).

15 Reluga, T. C., Dahari, H. & Perelson, A. S. Analysis of hepatitis C virus infection models with hepatocyte homeostasis. *SIAM J Appl Math* **69**, 999-1023, doi:10.1137/080714579 (2009).

16 Dahari, H., Shudo, E., Cotler, S. J., Layden, T. J. & Perelson, A. S. Modelling hepatitis C virus kinetics: the relationship between the infected cell loss rate and the final slope of viral decay. *Antiviral therapy* **14**, 459-464 (2009).

17 Dahari, H. *et al.* Pharmacodynamics of PEG-IFN-alpha-2a in HIV/HCV co-infected patients: implications for treatment outcomes. *J Hepatol* **53**, 460-467, doi:10.1016/j.jhep.2010.03.019 (2010).

18 Dahari, H., Rong, L., Layden, T. J. & Cotler, S. J. Hepatocyte proliferation and hepatitis C virus kinetics during treatment. *Clin Pharmacol Ther* **89**, 353-354, doi:10.1038/clpt.2010.238 (2011).

19 Saltzman, J., Nachbar, R., Panochorchan, P., Stone, J. & Khan, A. in *2009 SIAM Conference on "Mathematics for Industry"* (eds D. A. Fields & T. J. Peters) 73-83 (Society for Industrial and Applied Mathematics, 2010).

20 Reddy, M. B. *et al.* Pharmacokinetic/pharmacodynamic predictors of clinical potency for hepatitis C virus nonnucleoside polymerase and protease inhibitors. *Antimicrob. Agents Chemother.* **56**, 3144-3156, doi:10.1128/AAC.06283-11 (2012).

21 Nguyen, T. H. T., Mentré, F., Yu, J., Levi, M. & Guedj, J. A pharmacokinetic - viral kinetic model describes the effect of alisporivir monotherapy or in combination with peg-IFN on hepatitis C virologic response. *Clinl Pharm Ther* **96**, 599-608 (2014).

22 Nguyen, T. H. T. & Guedj, J. HCV kinetic models and thier implication in drug development. *Clinical pharmacology and therapeutics* (in press).

23 Dixit, N. M. & Perelson, A. S. The metabolism, pharmacokinetics and mechanisms of antiviral activity of ribavirin against hepatitis C virus. *Cell Mol. Life Sci.* **63**, 832-842, doi:10.1007/s00018-005-5455-y (2006).

24 Feld, J. J. Is there a role for ribavirin in the era of hepatitis C virus direct-acting antivirals? *Gastroenterology* **142**, 1356-1359, doi:10.1053/j.gastro.2011.12.064 (2012).

25 Feld, J. J. *et al.* Ribavirin improves early responses to peginterferon through improved interferon signaling. *Gastroenterology* **139**, 154-162 e154, doi:10.1053/j.gastro.2010.03.037 (2010).

26 Rotman, Y. *et al.* Effect of ribavirin on viral kinetics and liver gene expression in chronic hepatitis C. *Gut* **63**, 161-169, doi:10.1136/gutjnl-2012-303852 (2014).

27 Thomas, E. *et al.* Ribavirin potentiates interferon action by augmenting interferon-stimulated gene induction in hepatitis C virus cell culture models. *Hepatology* **53**, 32-41, doi:10.1002/hep.23985 (2011).

28 Mihm, U., Herrmann, E., Sarrazin, C. & Zeuzem, S. Review article: predicting response in hepatitis C virus therapy. *Aliment. Pharmacol. Ther.* **23**, 1043-1054, doi:10.1111/j.1365-2036.2006.02863.x (2006).

29 Canini, L. *et al.* A pharmacokinetic/viral kinetic model to evaluate the treatment effectiveness of danoprevir against chronic HCV. *Antiviral therapy*, doi:10.3851/IMP2879 (2014).

30 Shudo, E., Ribeiro, R. M., Talal, A. H. & Perelson, A. S. A hepatitis C viral kinetic model that allows for time-varying drug effectiveness. *Antiviral therapy* **13**, 919-926 (2008).

31 Conway, J. M. & Perelson, A. S. A hepatitis C virus infection model with time-varying drug effectiveness: solution and analysis. *PLoS Comp Biol* **10**, e1003769, doi:10.1371/journal.pcbi.1003769 (2014).

32 Shudo, E., Ribeiro, R. M. & Perelson, A. S. Modeling hepatitis C virus kinetics under therapy using pharmacokinetic and pharmacodynamic information. *Expert Opin Drug Metab Toxicol* **5**, 321-332, doi:10.1517/17425250902787616 (2009).

33 Guedj, J. & Perelson, A. S. Second-phase hepatitis C virus RNA decline during telaprevir-based therapy increases with drug effectiveness: implications for treatment duration. *Hepatology* **53**, 1801-1808, doi:10.1002/hep.24272 (2011).

34 Guedj, J., Dahari, H., Shudo, E., Smith, P. & Perelson, A. S. Hepatitis C viral kinetics with the nucleoside polymerase inhibitor mericitabine (RG7128). *Hepatology* **55**, 1030-1037, doi:10.1002/hep.24788 (2012).

35 Guedj, J. *et al.* Analysis of the hepatitis C viral kinetics during administration of two nucleotide analogues: sofosbuvir (GS-7977) and GS-0938. *Antivir. Ther. (Lond.)* **19**, 211-220, doi:10.3851/IMP2733 (2014).

36 Canini, L. *et al.* Severity of liver disease affects HCV kinetics in patients treated with intravenous silibinin monotherapy. *Antivir. Ther. (Lond.)* **in press**, doi:10.3851/IMP2806 (2015).

37 Canini, L. & Perelson, A. S. Viral kinetic modeling: state of the art. *J Pharmacokin Pharmacodyn* **41**, 431-433, doi:10.1007/s10928-014-9363-3 (2014).

38 Gao, M. *et al.* Chemical genetics strategy identifies an HCV NS5A inhibitor with a potent clinical effect. *Nature* **465**, 96-100, doi:10.1038/nature08960 (2010).

39 Guedj, J. *et al.* Modeling shows that the NS5A inhibitor daclatasvir has two modes of action and yields a shorter estimate of the hepatitis C virus half-life. *Proc Natl Acad Sci USA* **110**, 3991-3996, doi:10.1073/pnas.1203110110 (2013).

40 Neumann, A. U. *et al.* Differences in viral dynamics between genotypes 1 and 2 of hepatitis C virus. *J. Infect. Dis.* **182**, 28-35, doi:10.1086/315661 (2000).

41 Rong, L. *et al.* Analysis of hepatitis C virus decline during treatment with the protease inhibitor danoprevir using a multiscale model. *PLoS Comp Biol* **9**, e1002959, doi:10.1371/journal.pcbi.1002959 (2013).

42 Rong, L. & Perelson, A. S. Mathematical analysis of multiscale models for hepatitis C virus dynamics under therapy with direct-acting antiviral agents. *Math Bioscences* **245**, 22-30, doi:10.1016/j.mbs.2013.04.012 (2013).

43 Adiwijaya, B. S. *et al.* Rapid decrease of wild-type hepatitis C virus on telaprevir treatment. *Antiviral therapy* **14**, 591-595 (2009).

44 McGivern, D. R. *et al.* Kinetic analyses reveal potent and early blockade of hepatitis C virus assembly by NS5A inhibitors. *Gastroenterology* **147**, 453-462 e457, doi:10.1053/j.gastro.2014.04.021 (2014).

45 McGivern, D. R. *et al.* Protease inhibitors block multiple functions of the NS3/4A protease-helicase during the hepatitis C virus life cycle. *J Virol*, doi:10.1128/JVI.03188-14 (2015).

46 Meredith, L. W., Farquhar, M. J., Tarr, A. W. & McKeating, J. A. Type I interferon rapidly restricts infectious hepatitis C virus particle genesis. *Hepatology* **60**, 1891-1901, doi:10.1002/hep.27333 (2014).

47 Dahari, H., Ribeiro, R. M., Rice, C. M. & Perelson, A. S. Mathematical modeling of subgenomic hepatitis C virus replication in Huh-7 cells. *J. Virol.* **81**, 750-760, doi:10.1128/JVI.01304-06 (2007).

48 Binder, M. *et al.* Replication vesicles are load- and choke-points in the hepatitis C virus lifecycle. *PLoS pathogens* **9**, doi:10.1371/journal.ppat.1003561 (2013).

49 Snoeck, E. *et al.* A comprehensive hepatitis C viral kinetic model explaining cure. *Clinical pharmacology and therapeutics* **87**, 706-713, doi:10.1038/clpt.2010.35 (2010).

50 Reesink, H. W. *et al.* Rapid HCV-RNA decline with once daily TMC435: a phase I study in healthy volunteers and hepatitis C patients. *Gastroenterology* **138**, 913-921, doi:10.1053/j.gastro.2009.10.033 (2010).

51 Blight, K. J., McKeating, J. A. & Rice, C. M. Highly permissive cell lines for subgenomic and genomic hepatitis C virus RNA replication. *J Virol* **76**, 13001-13014 (2002).

52 Robinson, M. *et al.* Novel hepatitis C virus reporter replicon cell lines enable efficient antiviral screening against genotype 1a. *Antimicrob Agents Chemother* **54**, 3099-3106, doi:10.1128/AAC.00289-10 (2010).

53 Farley, S. A double whammy for hep C. *Nature Rev Drug Discovery* **2**, 419 (2003).

54 Liang, Y. *et al.* Antiviral suppression vs restoration of RIG-I signaling by hepatitis C protease and polymerase inhibitors. *Gastroenterology* **135**, 1710-1718 e1712, doi:10.1053/j.gastro.2008.07.023 (2008).

55 Guedj, J., Dahari, H., Shudo, E., Smith, P. & Perelson, A. S. Hepatitis C viral kinetics with the nucleoside polymerase inhibitor mericitabine (RG7128). *Hepatology* **55**, 1030-1037, doi:10.1002/hep.24788 (2012).

56 Osinusi, A. *et al.* Sofosbuvir and ribavirin for hepatitis C genotype 1 in patients with unfavorable treatment characteristics: a randomized clinical trial. *JAMA* **310**, 804-811, doi:10.1001/jama.2013.109309 (2013).

57 Adiwijaya, B. S. *et al.* A viral dynamic model for treatment regimens with direct-acting antivirals for chronic hepatitis C infection. *PLoS Comp. Biol.* **8**, e1002339, doi:10.1371/journal.pcbi.1002339 (2012).

58 Centro, V. *et al.* Kinetics of hepatitis C virus RNA decay, quasispecies evolution and risk of virological failure during telaprevir-based triple therapy in clinical practice. *Digestive Liver Dis.* **47**, 233-241 (2015).

59 Guedj, J. & Neumann, A. U. Understanding hepatitis C viral dynamics with direct-acting antiviral agents due to the interplay between intracellular replication and cellular infection dynamics. *J Theor Biol* **267**, 330-340, doi:10.1016/j.jtbi.2010.08.036 (2010).

60 Laouenan, C. *et al.* Using pharmacokinetic and viral kinetic modeling to estimate the antiviral effectiveness of telaprevir, boceprevir, and pegylated interferon during triple therapy in treatment-experienced hepatitis C virus-infected cirrhotic patients. *Antimicrob Agents Chemother* **58**, 5332-5341, doi:10.1128/AAC.02611-14 (2014).

61 Gane, E. J. *et al.* Oral combination therapy with a nucleoside polymerase inhibitor (RG7128) and danoprevir for chronic hepatitis C genotype 1 infection (INFORM-1): a randomised, double-blind, placebo-controlled, dose-escalation trial. *Lancet* **376**, 1467-1475, doi:10.1016/S0140-6736(10)61384-0 (2010).

62 Gane, E. J. *et al.* Mericitabine and ritonavir-boosted danoprevir with or without ribavirin in treatment-naive HCV genotype 1 patients: INFORM-SVR study. *Liver Intl.*, doi:10.1111/liv.12588 (2014).

63 Kowdley, K. V. *et al.* Ledipasvir and sofosbuvir for 8 or 12 weeks for chronic HCV without cirrhosis. *N. Engl. J. Med.* **370**, 1879-1888, doi:10.1056/NEJMoa1402355 (2014).

64 Sulkowski, M. *et al.* Efficacy and safety of 8 weeks versus 12 weeks of treatment with grazoprevir (MK-5172) and elbasvir (MK-8742) with or without ribavirin in patients with hepatitis C virus genotype 1 mono-infection and HIV/hepatitis C virus co-infection (C-WORTHY): a randomised, open-label phase 2 trial. *Lancet*, doi:10.1016/S0140-6736(14)61793-1 (2014).

65 Kohli, A. *et al.* Virologic response after 6 week triple-drug regimes for hepatitis C: a proof-of-concept phase 2A cohort study. *Lancet* **385**, 1107-1113, doi:http://dx.doi.org/10.1016/S0140-6736(14)61228-9 (2015).

66 Colombatto, P. *et al.* Early and accurate prediction of Peg-IFNs/ribavirin therapy outcome in the individual patient with chronic hepatitis C by modeling the dynamics of the infected cells. *Clinical pharmacology and therapeutics* **84**, 212-215, doi:10.1038/clpt.2008.21 (2008).

67 Guedj, J. *et al.* Modeling viral kinetics and treatment outcome during alisporivir interferon-free treatment in HCV genotype 2/3 patients. *Hepatology* **59**, 1706-1714, doi:10.1002/hep.26989 (2014).

68 Kieffer, T. L. *et al.* Telaprevir and pegylated interferon-alpha-2a inhibit wild-type and resistant genotype 1 hepatitis C virus replication in patients. *Hepatology* **46**, 631-639, doi:10.1002/hep.21781 (2007).

69 Ribeiro, R. M. *et al.* Quantifying the diversification of hepatitis C virus (HCV) during primary infection: estimates of the in vivo mutation rate. *PLoS pathogens* **8**, e1002881, doi:10.1371/journal.ppat.1002881 (2012).

70 Cuevas, J. M., González-Candelas, F., Moya, A. & Sanjuán, R. Effect of ribavirin on the mutation rate and spectrum of hepatitis C virus in vivo. *J. Virol.* **83**, 5760-5764, doi:10.1128/JVI.00201-09 (2009).

71 Rong, L., Dahari, H., Ribeiro, R. M. & Perelson, A. S. Rapid emergence of protease inhibitor resistance in hepatitis C virus. *Sci. Trans. Med.* **2**, 30ra32, doi:10.1126/scitranslmed.3000544 (2010).

72 Adiwijaya, B. S. *et al.* A multi-variant, viral dynamic model of genotype 1 HCV to assess the in vivo evolution of protease-inhibitor resistant variants. *PLoS computational biology* **6**, doi:10.1371/journal.pcbi.1000745 (2010).

73 Haseltine, E. L. *et al.* Modeling viral evolutionary dynamics after telaprevir-based treatment. *PLoS Comp. Biol.* **10**, e1003772 (2014).

74 Greco, W. R., Bravo, G. & Parsons, J. C. The search for synergy: a critical review from a response surface perspective. *Pharmacol. Rev.* **47**, 331-385 (1995).

75 Lee, J. J., Kong, M., Ayers, G. D. & Lotan, R. Interaction index and different methods for determining drug interaction in combination therapy. *J. Biopharm. Stat.* **17**, 461-480, doi:10.1080/10543400701199593 (2007).

76 Cheng, G. *et al.* Antiviral activity and resistance profile of the novel HCV NS5A inhibitor GS-5885. *47th Annual Meeting of the European Association for the Study of the Liver* **Poster No. 1172** (2012).

77 Sarrazin, C. & al., e. Importance of very early HCV RNA kinetics for prediction of treatment outcome of highly effective all oral direct-acting antiviral combination therapy. *J Virol Methods* (in press).

78 Sidharthan, S. *et al.* Utility of hepatitis C viral load monitoring on directly acting antiviral therapy. *Clin. Infect. Dis.* **in press**, doi:10.1093/cid/civ170 (2015).

79 Saez-Cirion, A. *et al.* Post-treatment HIV-1 controllers with a long-term virological remission after the interruption of early initiated antiretroviral therapy ANRS VISCONTI Study. *PLoS pathogens* **9**, e1003211, doi:10.1371/journal.ppat.1003211 (2013).

80 Lawitz, E. *et al.* A phase 2a trial of 12-week interferon-free therapy with two direct-acting antivirals (ABT-450/r, ABT-072) and ribavirin in IL28B C/C patients with chronic hepatitis C genotype 1. *J Hepatol* **59**, 18-23, doi:10.1016/j.jhep.2013.02.009 (2013).

81 Soriano, V. *et al.* Very late relapse after discontinuation of antiviral therapy for chronic hepatitis C. *Antiviral therapy* **18**, 1033-1035, doi:10.3851/IMP2659 (2013).

82 Barreiro, P. *et al.* Very late HCV relapse following triple therapy for hepatitis C. *Antiviral therapy* **19**, 723-724, doi:10.3851/IMP2753 (2014).

83 Veerapu, N. S., Raghuraman, S., Liang, T. J., Heller, T. & Rehermann, B. Sporadic reappearance of minute amounts of hepatitis C virus RNA after successful therapy stimulates cellular immune responses. *Gastroenterology* **140**, 676-685 e671, doi:10.1053/j.gastro.2010.10.048 (2011).

84 Lin, J. C. *et al.* Interferon γ-induced protein 10 kinetics in treatment-naive versus treatment-experienced patients receiving interferon-free therapy for hepatitis C virus infection: Implications for the innate immune response. *J Infect Dis* **10**, 1881-1885, doi:10.1093/infdis/jiu325 (2014).

85 *Food and Drug Administration Center for Drug Evaluation Research. Guidance for Industry Chronic Hepatitis C Virus Infection: Developing Direct-Acting Antiviral Drugs for Treatment (Draft)*, <http://www.fda.gov/downloads/drugs/guidancecomplianceregulatoryinformation/guidances/ucm225333.pdf> (2013).

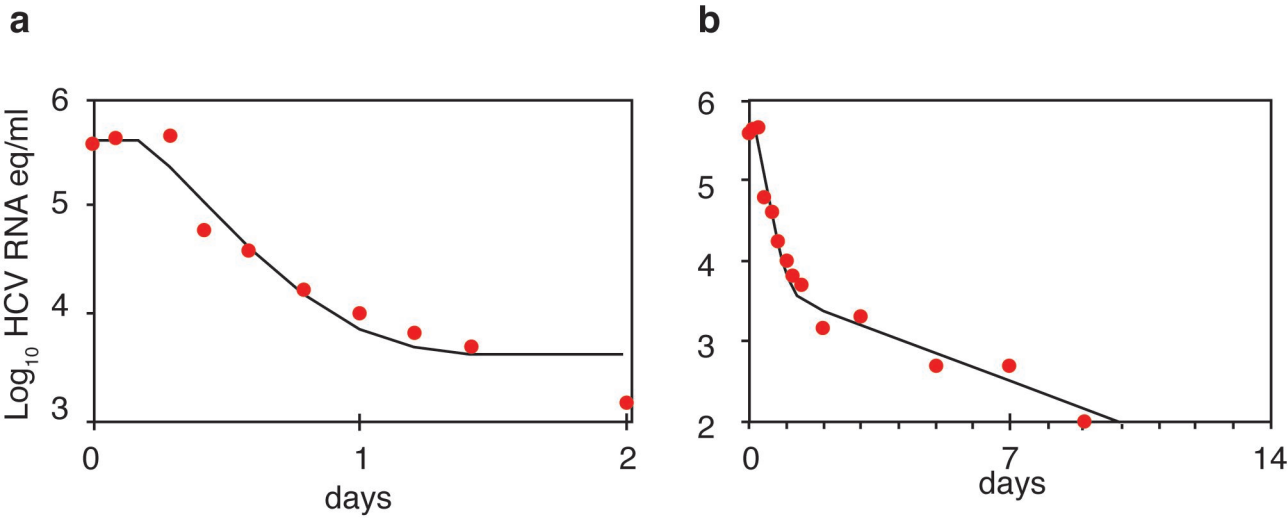
a
b
Log10 HCV RNA eq/ml
6
5
4
3
2
0
1
2
7
14
days
days

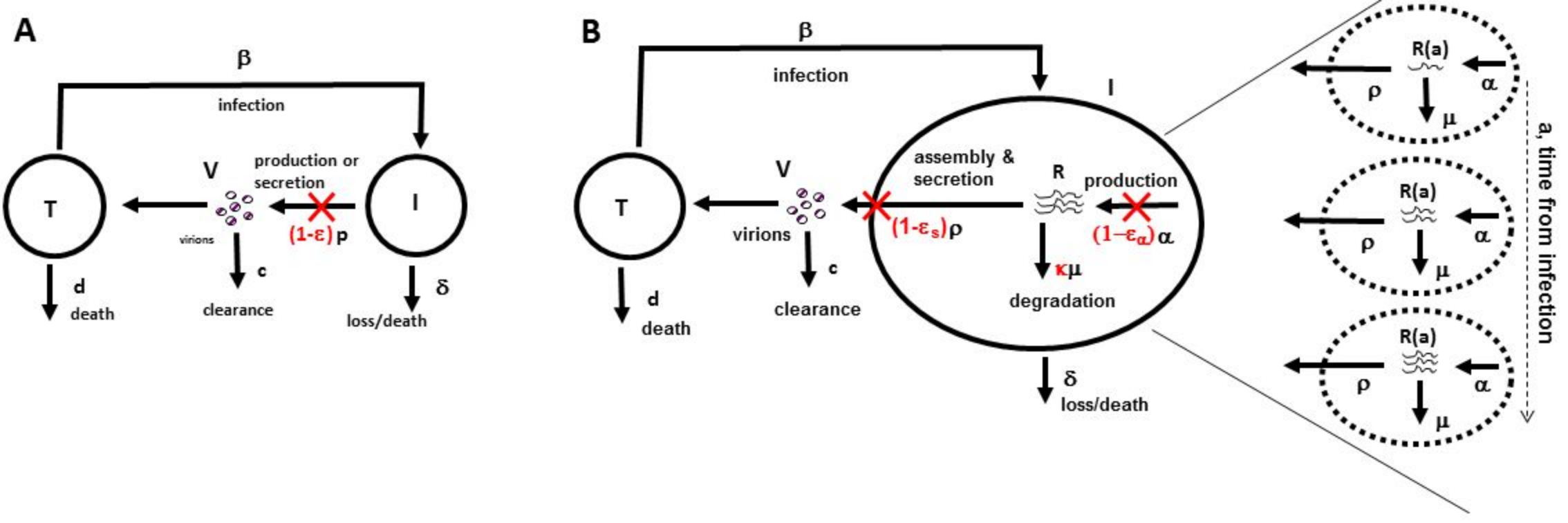
A
β
infection
T
V
virions
production or
secretion
(1-ε) p
I
d
death
c
clearance
δ
loss/death
B
β
infection
I
T
V
virions
assembly &
secretion
(1-ε_s) ρ
R
production
(1−ε_α) α
κμ
degradation
d
death
c
clearance
δ
loss/death
R(a)
ρ
α
μ
a, time from infection

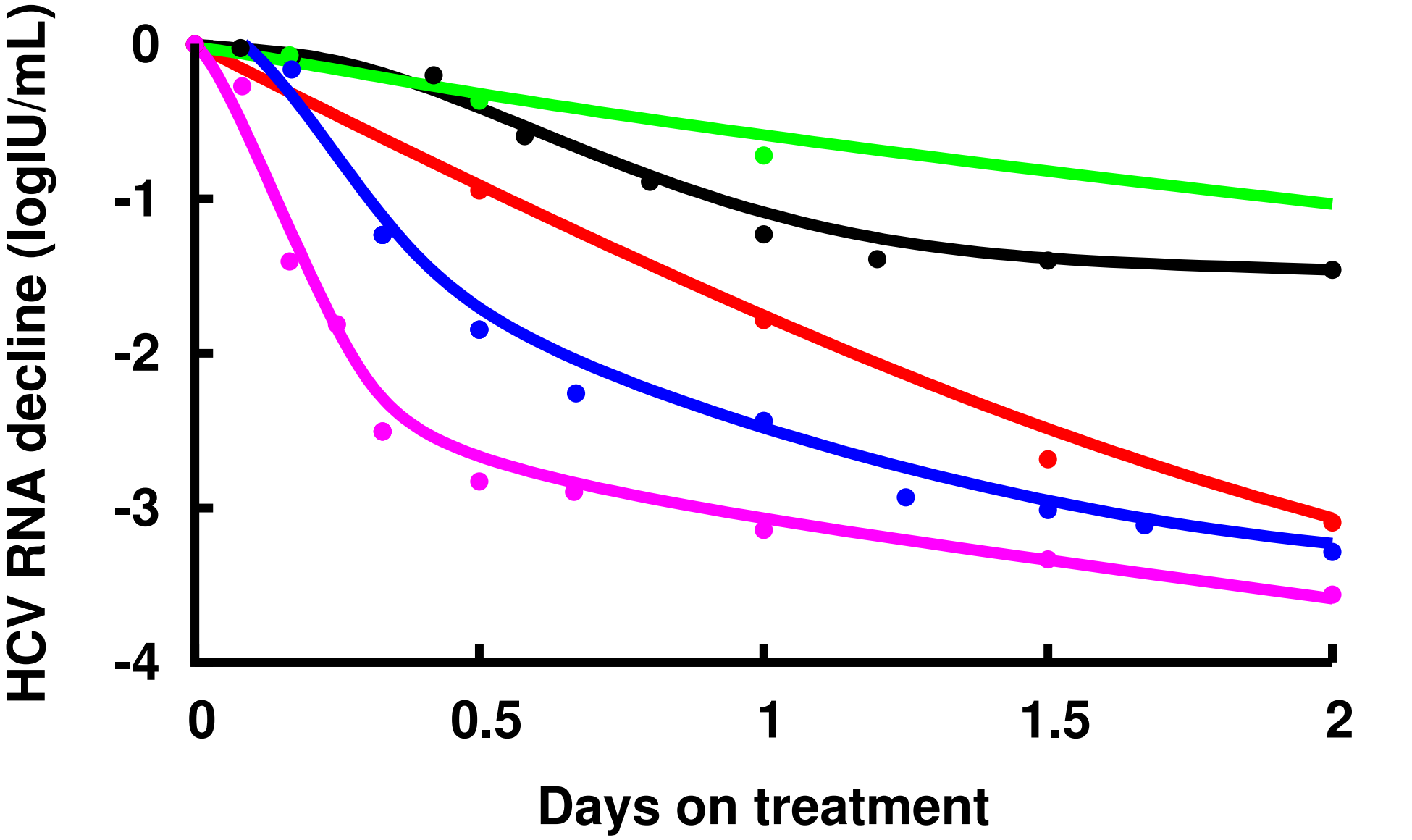
HCV RNA decline (logIU/mL)
0
-1
-2
-3
-4
0
0.5
1
1.5
2
Days on treatment

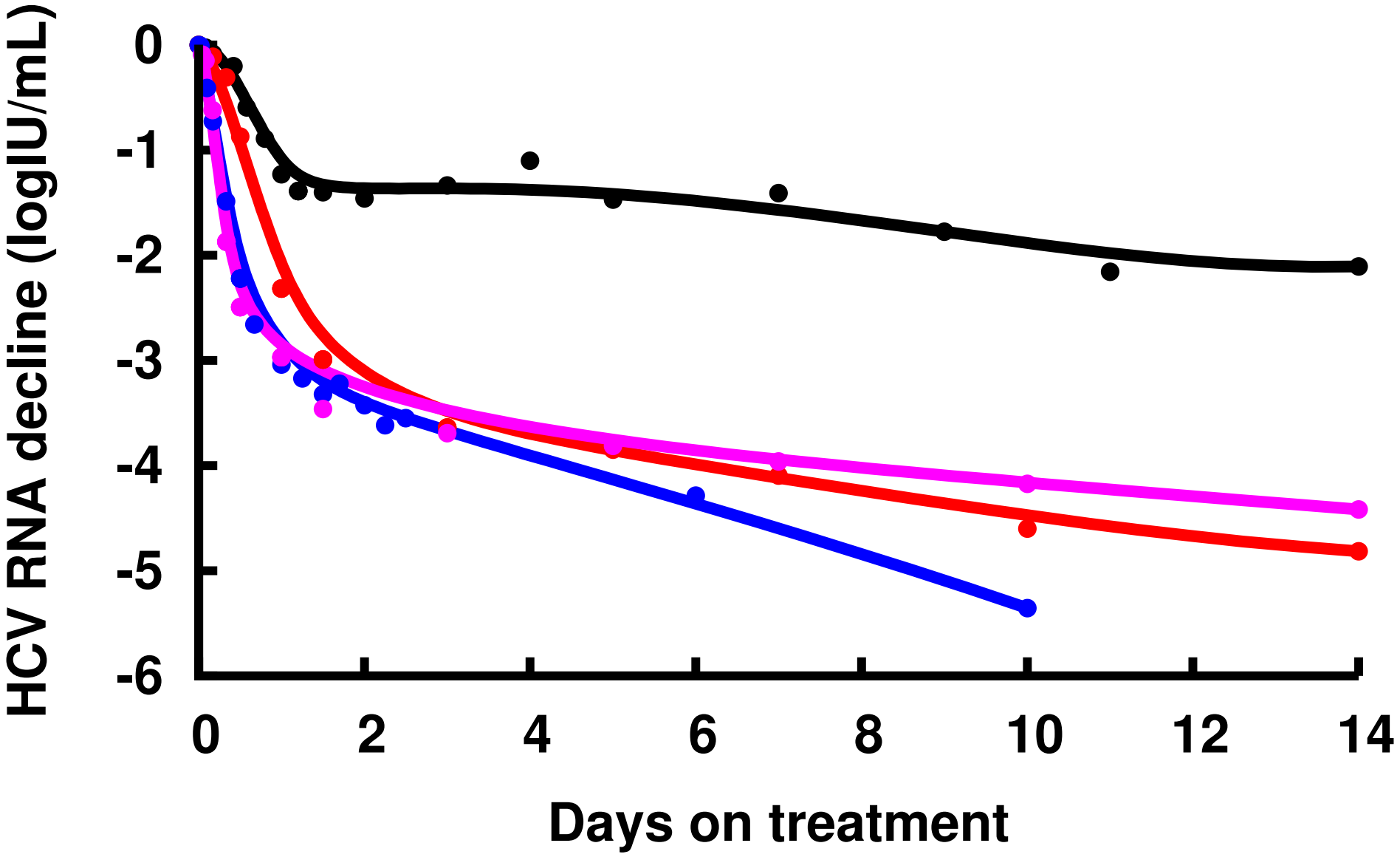
HCV RNA decline (logIU/mL)
0
-1
-2
-3
-4
-5
-6
0
2
4
6
8
10
12
14
Days on treatment

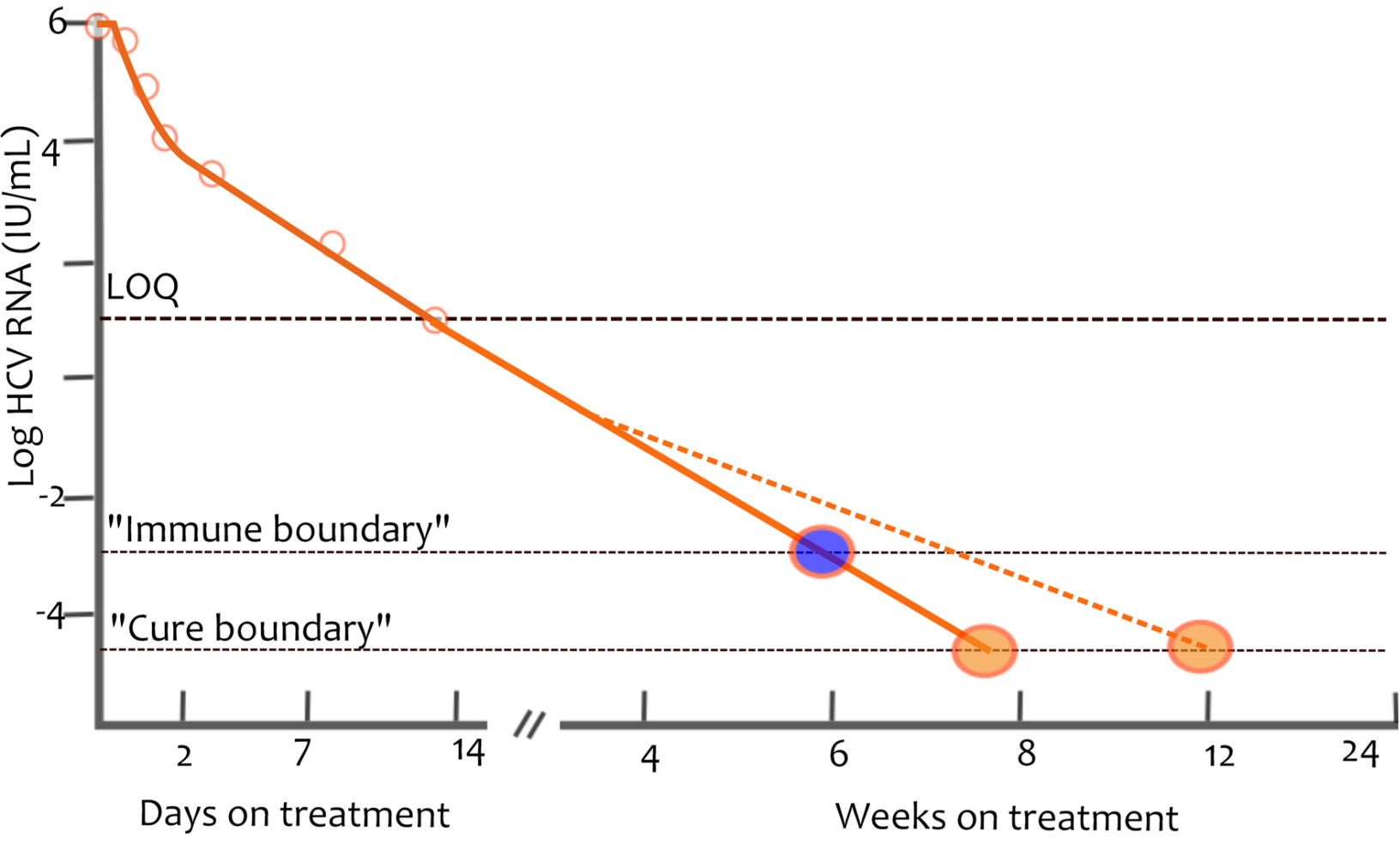
6
4
-2
-4
Log HCV RNA (IU/mL)
LOQ
"Immune boundary"
"Cure boundary"
2
7
14
4
6
8
12
24
Days on treatment
Weeks on treatment